Chinese Chemical Letters 37 (2026) 111902

Contents lists available at ScienceDirect

Chinese Chemical Letters

journal homepage: www.elsevier.com/locate/cclet

Recent development in fluorescent probes for monitoring organophosphorus pollutants

Kun Song[a,1], Lijia Zhang[a,1], Yunhui Meng[a], Jiantong Ding[a], Xiaobai Li[a,*], Yongpeng Liu[c,*], Hongwei Ma[a,b,*]

[a] Department of Chemistry and Chemical Engineering, College of Chemistry, Chemical Engineering and Resource Utilization, Northeast Forestry University, Harbin 150040, China
[b] Heilongjiang Key Laboratory of Complex Traits and Protein Machines in Organisms, Northeast Forestry University, Harbin 150040, China
[c] Yusuf Hamied Department of Chemistry, University of Cambridge, Cambridge CB2 1EW, United Kingdom

ARTICLE INFO

Article history:
Received 2 July 2025
Revised 8 September 2025
Accepted 25 September 2025
Available online 26 September 2025

Keywords:
Organophosphorus pollutants
Analytical chemistry
Fluorescent probes
Reaction mechanisms
Design guidelines

ABSTRACT

Organophosphorus (OPs) compounds are extensively utilized in pesticides, chemical warfare agents, pharmaceuticals, and industrial applications due to their distinctive chemical properties, including biological activity, persistence, and hydrophobicity. However, their excessive use has led to significant environmental toxicity and pollution concerns, underscoring the urgent need for sustainable methods to monitor OPs pollutants. Traditional detection relies on bulky instruments, whereas organic fluorescent probes present advantages such as high selectivity, sensitivity, and portability. This review summarizes recent advancements in these probes for OPs detection, outlines characterization strategies based on underlying mechanisms, discusses challenges and future directions, and introduces OPs' features, probe mechanisms, and design guidelines, providing theoretical insights and technical references for the development of novel organic fluorescent probes.

© 2026 Published by Elsevier B.V. on behalf of Chinese Chemical Society and Institute of Materia Medica, Chinese Academy of Medical Sciences.

1. Introduction

Organophosphorus (OPs) compounds are a diverse class of chemicals characterized by the presence of carbon–phosphorus (C-P) bonds. Owing to their distinctive physicochemical properties such as high reactivity, lipophilicity, and structural diversity, OPs have found extensive applications across multiple domains. In agriculture, they are widely used as active ingredients in pesticides and herbicides [1]. In the military, certain OPs serve as the chemical basis for nerve agents [2]. And in industry, they are utilized in flame retardants, plasticizers, and lubricants [3]. However, the extensive use of OPs has led to their widespread distribution in air, soil, and water, raising serious environmental and public health concerns [4]. Due to their lipophilicity, OPs pollutants exhibit high toxicity and environmental persistence, posing serious risks to human health and ecosystems. Their accumulation in the food chain can cause diseases in animals and plants, while exposure to nerve agents may result in acute toxicity and mortality in wildlife. Industrial leakage of OPs further contributes to environmental contamination and ecological disruption [5].

Accurate detection of OPs pollutants is a critical first step in environmental remediation. Conventional detection methods, such as gas or liquid chromatography-mass spectrometry and Raman spectroscopy, rely on bulky, complex instrumentation, limiting their portability and suitability for rapid on-site analysis [6]. Biological probe-based techniques often require sophisticated materials and technologies, with limited flexibility once designed, restricting their applicability across diverse detection scenarios [7]. Moreover, enzyme-based probes are prone to loss of activity under varying environmental conditions, compromising their stability in complex matrices. In contrast, organic fluorescent probes as emerging technologies offer well-defined molecular structures, enabling precise control over sensing performance. They also exhibit superior biocompatibility, reducing the risk of secondary environmental contamination, and their relatively simple synthesis results in lower research and development costs [8,9]. The development of organic fluorescent probes for detecting OPs pollutants has grown rapidly in recent years, as evidenced by a sharp increase in related citations: from approximately 2000 in 2015 to nearly 5500 in 2024 (Fig. 1).

* Corresponding authors.
E-mail addresses: lixiaobai2008@126.com (X. Li), yl862@cam.ac.uk (Y. Liu), mahw@nefu.edu.cn (H. Ma).
[1] These authors contributed equally to this work.

https://doi.org/10.1016/j.cclet.2025.111902
1001-8417/© 2026 Published by Elsevier B.V. on behalf of Chinese Chemical Society and Institute of Materia Medica, Chinese Academy of Medical Sciences.

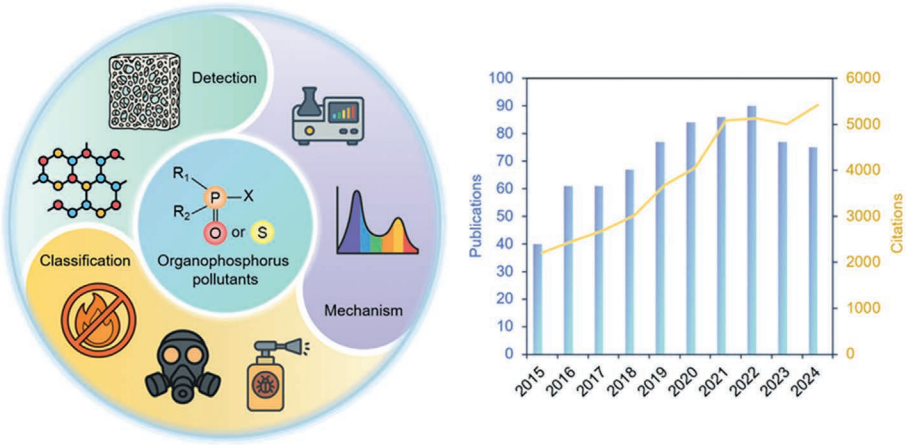


Fig. 1. Organic fluorescent probes for the detection of OPs pollutants and annual publications and citations on OPs detection using fluorescent probes (assessed 4 May, 2025).

This review presents a comprehensive analysis of recent advances in design strategies and performance optimization of organic fluorescent probes for the detection of OPs pollutants. The probes are categorized according to their underlying photophysical mechanisms, offering insights into structure–property relationships that govern their sensing behavior. In addition, the developmental trajectory from molecular design to functional characterization is examined, highlighting key factors that influence sensitivity, selectivity, and environmental stability. By integrating these findings, the review provides valuable theoretical references and technical guidance to support the rational design of next-generation fluorescent sensing platforms for OPs pollutant detection.

2. Overview of OPs pollutants

OPs pollutants comprise a diverse class of compounds characterized by phosphorus–oxygen or phosphorus–sulfur double bonds and a variety of organic substituents, whose widespread use has given rise to significant environmental and health concerns [10]. Organophosphorus pesticides (OPPs) are among the most prevalent OPs in modern agriculture, valued for their high efficacy and cost-effectiveness but notorious for contaminating soil and water and bioaccumulating in the food chain [11]. Organophosphorus nerve agents (OPNAs), originally developed for military applications, possess extreme toxicity and volatility [12]; even minute exposures can cause acute cholinergic crises and have been misused in chemical warfare and terrorist attacks. Organophosphorus flame retardants (OPFRs) serve as non-halogenated substitutes for brominated flame retardants in plastics, textiles, and electronics [13]; although designed for lower acute toxicity, their persistence and potential endocrine-disrupting effects have raised new regulatory and remediation challenges.

2.1. Classification

OPs compounds constitute a diverse class of phosphoric or thiophosphoric acid esters and amides, each centered on a phosphorus (P) atom. This P center is typically double-bonded to either an oxygen (P=O) or a sulfur (P=S) atom and singly bonded to a combination of alkoxy, aryloxy, amino, or thioalkoxy substituents (R and R' groups). This structural versatility, enabled by the incorporation of various heteroatoms such as oxygen (O), nitrogen (N), and sulfur (S), imparts a wide range of physicochemical properties and reactivity profiles to OPs [14]. The P=O bond, commonly found in OPNAs, exhibits heightened electrophilicity, strong polarity, and high reactivity, which facilitates its efficient binding to the nucleophilic moieties of probes. In contrast, the P=S bond, characterized by relatively low polarity and prevalent in OPPs, engages in weaker interactions with probes, necessitating the design of more specific recognition sites to prevent interference. Furthermore, steric hindrance caused by bulky aromatic substituents in OPFRs limits their interaction with small-molecule probes, while the length of alkyl chains influences the sensitivity of fluorescent probes (Fig. 2).

OPPs are broad-spectrum insecticides [15]. They can be classified according to their toxicity into three categories: highly toxic, moderately toxic, and low toxic. Highly toxic pesticides include ethyl-parathion (EP), omethoate (OMT), disulfoton (DST), and paraoxon, moderately toxic pesticides include chlorpyrifos (CPF), dichlorvos (DDVP), methyl-parathion (MP) and diazinon, low toxic pesticides include glyphosate (GLP), dimethoate (DMT), malathion (MLT), and chlorthion (OMS) [16]. Among these, there are OPPs with low flash points that are both flammable and explosive [17], as well as those that are highly soluble in water and can contaminate aquatic environments (Table S1 in Supporting information).

OPNAs are highly toxic chemical warfare agents (CWAs). Their extreme toxicity can result in severe consequences even at low exposure levels, raising widespread global concern [18]. Additionally, OPNAs are a significant component of sea-dumped chemical weapons [19]. Over time, the casings of these chemical weapons may corrode due to various factors, leading to the leakage of chemical agents into water, soil, or plants [20]. This not only causes significant environmental pollution but also poses long-term potential hazards to both the ecosystem and human health. OPNAs are typically classified into three categories: G series, V series, and A series (Table S2 in Supporting information) [21].

In addition to OPPs and OPNAs, various other organophosphate compounds have garnered significant attention. These include, but are not limited to, organophosphates, organophosphate flame retardants, and organophosphate plasticizers [22]. OPs flame retardants (OPFRs) are increasingly recognized as hazardous OPs pollutants [23]. They are highly bio-toxic and leading to irreversible damage to both human health and the ecosystem [24]. Currently, the primary OPs flame retardants detected using fluorescent methods include tris(2-chloroethyl)phosphate (TCEP), tricresyl phosphate (TCP), and triphenyl phosphate (TPHP).

2.2. Toxicity

OPs' acute toxicity stems mainly from irreversible covalent phosphorylation of serine hydroxyls in acetylcholinesterase's (AChE) active site (Fig. 3a) [25]. Serines' O-H donates electrons to OP's phosphorus, displacing a leaving group to form a phosphoester. Phosphorylated AChE can't hydrolyze acetylcholine (ACh),

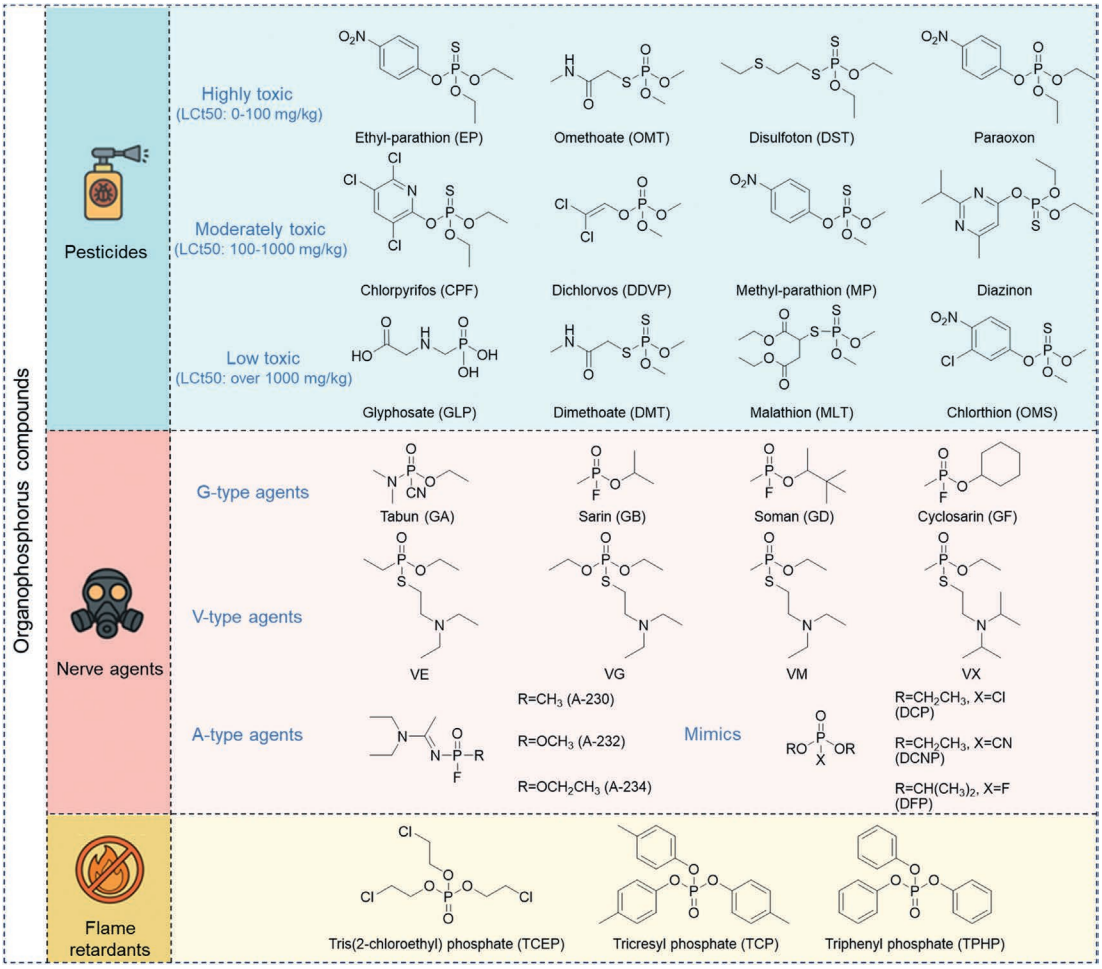


Fig. 2. Structural formulae of the three most common OPs pollutants: pesticides, nerve agents, and flame retardants.

causing its synaptic buildup [26]. However, some studies show OPs are toxic even below AChE inhibition thresholds, *via* non-cholinergic mechanisms, such as causing oxidative stress through glutathione depletion, lipid peroxidation, and excess reactive oxygen species (ROS) [27,28]. Meanwhile, certain OPs pollutants can interfere with neural axonal transport, directly contributing to neurodegenerative pathologies (Fig. 3b) [29].

3. Detection of OPs pollutants using organic fluorescent probes

3.1. Organic fluorescent probes

Organic fluorescent probes are divided into organic small molecule fluorescent probes and organic polymer fluorescent probes according to molecular weight. Fluorescent probe models can also be classified as switching or ratiometric, depending on the characteristics of the fluorescence signal changes [30]. In the early stages of fluorescent probe design, quench probes of the switching type predominated. When characterizing the mechanism of interaction between the quencher and the fluorescent substance, two types of quenching can be identified: static and dynamic quenching. These types can be distinguished by whether the quencher affects the lifetime of the fluorescent substance [31]. Static quenching occurs when a non-fluorescent complex forms between the quencher and the fluorescent substance. Consequently, the presence of a quencher during static quenching does not influence the fluorescence lifetime of the fluorescent substance. With advancements in theory and technology, there is an increasing trend toward the development of improved fluorescent probes. Their fluorescence changes are more discernible than those of quench fluorescent probes, providing more reliable results in practical applications. In contrast, ratiometric fluorescent probes rely on the combined variation of two fluorescent signals. Compared to single-emission fluorescent probes, ratiometric fluorescence probes significantly reduces interference from external environmental factors and enhances selectivity to a certain extent [32]. Additionally, ratiometric fluorescent probes provide richer colorimetric information for visual inspection, resulting in more accurate visual sensing outcomes.

3.2. Mechanism

The common mechanisms of interaction between fluorescent probes and detection substances include photoinduced electron transfer (PET), intramolecular charge transfer (ICT), fluorescence resonance energy transfer (FRET), inner-filter effect (IFE), excited state intramolecular proton transfer (ESIPT), and de-hybridization of hybrid local and charge transfer (De-HLCT) [33].

The PET mechanism plays a fundamental role in the fluorescence detection of organic phosphorus compounds, particularly in the detection of OPNAs. This mechanism involves atoms with lone pair electron atoms such as O, N, S, Se. And this mechanism is based on advanced molecular orbital theory, which is categorized into two types: a-PET and d-PET (Fig. 4a) [34]. It is worth noting that PET probes are often susceptible to interference from pH conditions during practical operations. This susceptibility arises from

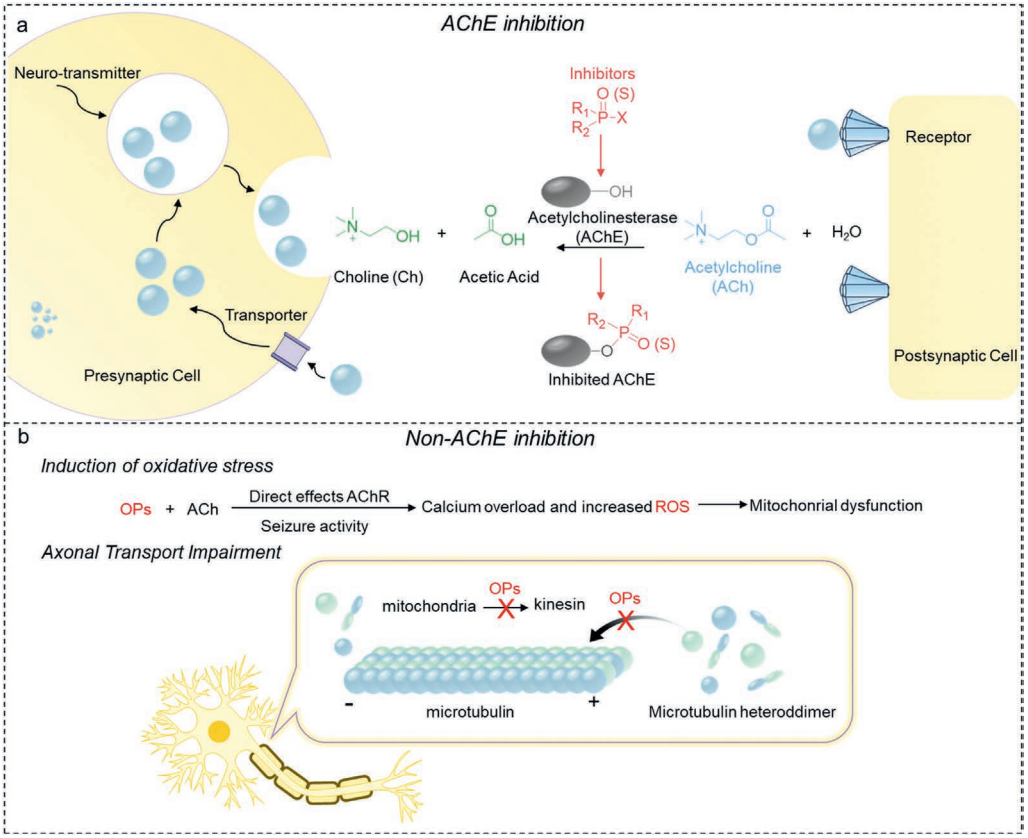


Fig. 3. Basic schematic of the mechanism of toxicity induced by OPs.

the interaction between protons and individual atoms within the probe [35]. Additionally, the presence of electron donors can readily induce electron transfer, complicating the ability of PET probes to consistently achieve optimal background fluorescence.

ICT is a fundamental photochemical process that plays a crucial role in the design of ratiometric fluorescent probes. Fluorescent probes that utilize the ICT mechanism effectively address the limitations of PET mechanism in the development of ratio probes. However, to achieve optimal detection results, the emission peak generated by guest molecules in ICT probes must exhibit a sufficiently large displacement. In practical applications, the ICT emission peak tends to be broad and the two emission peaks-before and after the response overlap significantly [36]. Furthermore, recognition groups typically contain multiple atoms with lone pair electrons (such as O, N, S), which can induce a PET effect, resulting in fluorescence quenching. After binding with the test substance, the PET effect will either weaken or disappear entirely, leading to a fluorescence redshift or blueshift in fluorescence, accompanied by an enhancement in fluorescence intensity. The new emission peak will completely overshadow the original emission peak, making ratio detection impractical (Fig. 4b). Therefore, not all ICT-based fluorescent probes are suitable for use as ratiometric fluorescent probes.

The FRET process involves the transfer of energy from the excited state of a donor fluorophore to the ground state of an acceptor fluorophore [37], mediated by electron dipole-dipole coupling. To reduce distance dependence and enhance energy transfer efficiency, the distance between the donor acceptor (D-A) should be maintained within the range of 10-100 Å (Fig. 4c). At the same time, the emission dipole moment of the donor, the absorption dipole moment of the acceptor, and their separation vectors must maintain a favorable mutual orientation. Furthermore, the emission spectrum of the donor and the absorption spectrum of the acceptor should overlap by more than 30 % to ensure effective energy transfer. Probe design can be optimized by adjusting the distance of the linker and the optical properties of the receptor. The IFE process is considered a physical interference phenomena in fluorescence measurements [38]. However, because IFE does not require any electron or energy transfer processes, it is more flexible and straightforward compared to FRET-based or PET-based fluorescence methods, which involve connections between the absorber and the fluorophore (Fig. 4d).

The ESIPT process is a unique four-stage photochemical phenomenon characterized by an extremely rapid enol-to-ketone photo-interchange process, which occurs through the redistribution of the electronic charge of the molecule upon light excitation [39]. ESIPT fluorophores exhibit significantly larger Stokes shifts compared to conventional fluorophores, effectively minimizing unwanted self-reabsorption and internal filtering effects (Fig. 4e) [40]. As a result, a diverse array of ESIPT fluorescent probes has emerged in recent years for the detection of organic pollutants [41].

Generally, the charge transfer (CT) state in the system exhibits weaker binding energy compared to the localized excited (LE) state excitons and is more sensitive to external stimuli [42]. However, the CT state has a lower radiative transition rate, which results in reduced fluorescence brightness of the molecular system when emitting light in the CT state compared to the LE state emission system. To integrate the characteristics of these two excited states, it is possible to cleverly utilize the de-HLCT excited states for detection (Fig. 4f).

In addition to the mechanism of excited state, the selection of organic functional groups is also crucial for the detection of OPs. Some of the more common responsive groups among them (Fig. 5) primarily occur at three sites: N-group reactive sites, O-group reac-

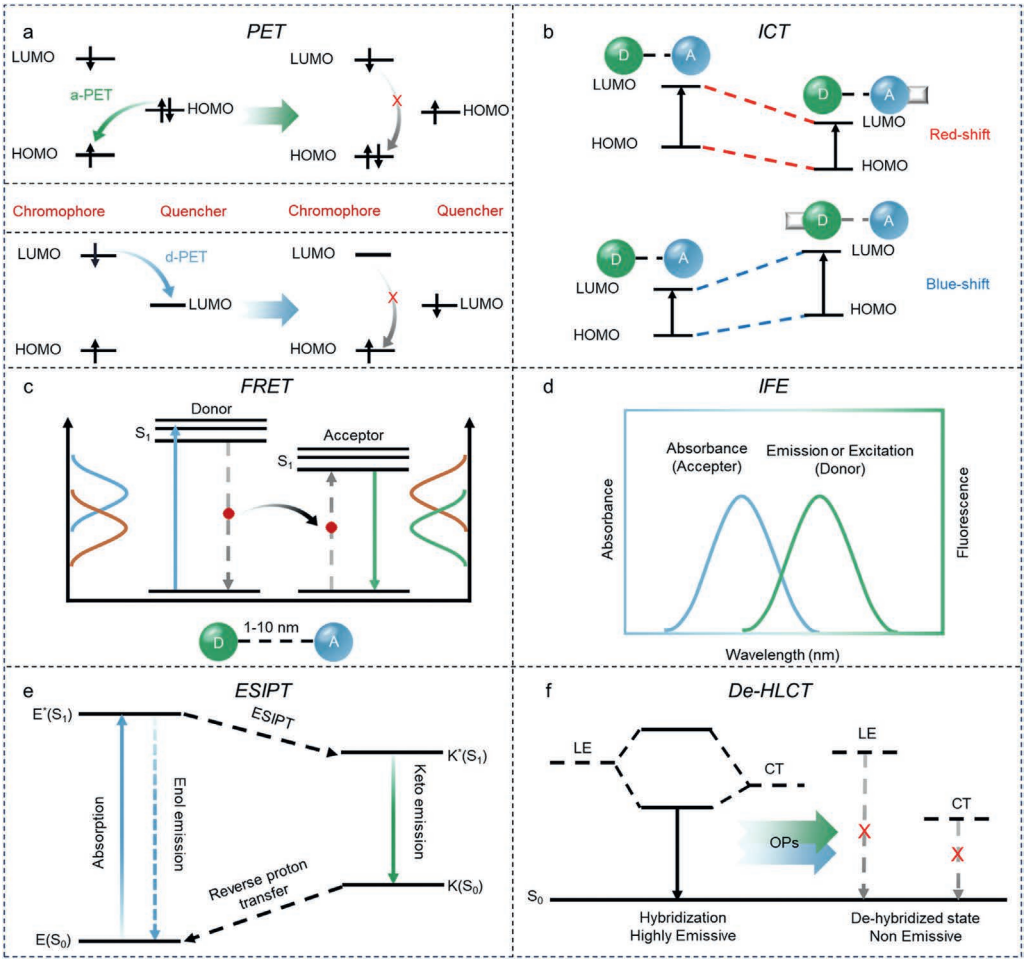


Fig. 4. Fluorescent probes detection mechanism based on PET, ICT, FRET, IFE, ESIPT and De-HLCT process.

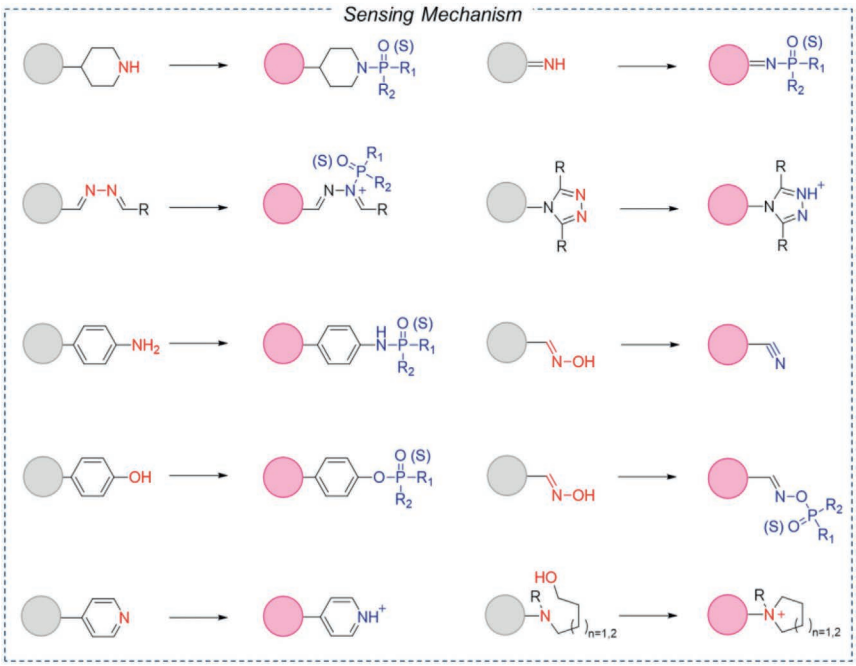


Fig. 5. A generalized chemical reaction-based fluorescence design strategy for the detection of OPs.

tive sites, and combined N- and O-group reactive sites [43]. Among these, nucleophilic reagent materials containing N-groups constitute an important class of fluorescent probes, which mainly include amines, pyridines, quinolines, and quinoxalines. N-Based nucleophilic reagents generally provide two mechanisms for detecting OPs. The first mechanism is a protonation process that enhances ICT effect while the second mechanism is a phosphorylation process that inhibits PET process. Both mechanisms result in significant alterations in the fluorescence of the probe molecule. The O-based nucleophilic reagents primarily consist of phenols. Phosphorylation of these phenolic compounds typically does not lead to substantial changes in the fluorescence of the sensing materials; however, the fluorescence may be affected when molecular rotation is induced by the phosphorylation of the chromophore. A variety of fluorescent materials have been developed for the detection of solutions using oxime-based nucleophilic recognition groups. These materials generally exhibit a fluorescence turn-on response and are synthesized by combining amino and hydroxyl groups to form oximes, which serve as recognition groups. Although alcohols exhibit stronger nucleophilicity than phenols, phosphorylation does not affect the π-conjugation or fluorescence of the sensing chromophore. However, alkyl alcohols can be integrated into fluorescent probes alongside pyridines, amines, and other compounds, serving as an effective strategy for designing fluorescent sensing materials. This is because the cyclization reaction following phosphorylation can produce novel structures with varying photoluminescent properties compared to the original sensing compounds.

3.3. Nerve agents

Organophosphorus nerve agents (OPNAs) are among the most potent chemical warfare agents ever developed. Structurally analogous to organophosphate pesticides, OPNAs such as tabun, sarin, soman and VX consist of a central phosphorus atom bonded to leaving groups that confer extreme electrophilicity. Consequently, sensing materials designed for their detection typically incorporate nucleophilic groups. The strategy for detecting OPNAs is commonly based on the following approach: nucleophilic groups attack phosphorus atoms, leading to the substitution of fluorine and chlorine atoms in the nerve agents. This interaction links the nerve agent to the sensing compound, resulting in observable changes in fluorescence. Another specific method for developing probes involves designing functionalized sensing compounds that coordinate with the P=O functional group, producing significant changes in fluorescence.

Small molecule fluorescent groups have been the focus of early research and development in the field of fluorescent probes, and they are widely utilized in the design of various types of fluorescent probes [44]. These fluorescent groups offer several advantages, including high quantum yield, straightforward synthesis, excellent biocompatibility, and ease of modification. The primary distinction between conjugated polymer systems and small molecule detection lies in the mechanisms of fluorescence quenching and the absence of exciton migration in small molecules. Polymer probes typically detect analytes through static quenching, whereas small molecules are generally quenched *via* collision [45]. Additionally, polymers exhibit a higher quenching efficiency, as a single binding analyte molecule can quench multiple excitons within the polymer. In contrast, small molecule fluorescent groups undergo quenching in a stoichiometric manner (Table 1).

Despite the alcohol hydroxyl group exhibiting strong nucleophilic properties, its phosphorylation process seldom alters the π-conjugated structure of the fluorophore, thereby rarely inducing fluorescence changes in probes. However, when a pyridine or aliphatic amine is present in the probe, the hydroxyl group may undergo an intramolecular cyclization reaction with the pyridine or amine group following phosphorylation. This reaction can modify the conjugated structure of the fluorophores, resulting in different fluorescence emissions. For instance, in 1998, Pilato *et al.* developed the first fluorescence probe **1**, based on a 1,2-ene dimercaptan complex, and subsequently applied it to the detection of phosphate esters such as, DCP and DFP [46]. Originally, a thin film mixture of probe **1** within cellulose acetate (CA) and 150% triethyl citrate exhibited minimal fluorescence emission. However, under alkaline conditions, the fluorescence emission of the film significantly increased after exposure to DCP or DFP vapor. It is important to note that the fluorescence of the cyclization product, probe **1-2**, can be easily quenched by oxygen molecules, necessitating the use of the **9** probe in a nitrogen atmosphere (Fig. 6a).

To avoid this defect, Swager *et al.* developed three fluorescent probes following with similar intramolecular cyclization reactions in 2003, numbered as probes **2-4** [47]. The probe **5**-CA mixed film exhibited a significant enhancement and red shift in its fluorescence spectra upon exposure to 10 ppm DFP within a few seconds (Fig. 6b), making it one of the most responsive probes to date.

However, hydrochloric acid still interferes with these probes to a certain extent. In 2018, Pilato developed a new probe **10** that can be used in the air (Fig. 6e) [48]. During this period, researchers synthesized numerous alcohol hydroxyl-based fluorescent probes **5**-**9** [49–52], with their structural formulas illustrated in Fig. 6. Among these, probe **9**, when adsorbed onto silica substrates, achieves a LOD of 0.2 ppm for DCNP vapor in real-world environments (Fig. 6f), demonstrating the practical potential of integrated films for field applications [53].

It is important to note that the response mechanisms of these probes are not identical. Probes **1**-**5** generate cyclization products upon contact with DCNP and DFP. The rigid structure of these cyclization products significantly reduces energy loss due to non-radiative transitions, thereby enhancing fluorescence emission. Interestingly, the fluorescence response of the polyoxyethylene ether-doped films based on BODIPY probes **6**-**9** to DCNP vapor was significantly superior to that of DFP and DCP (Fig. 6g). The exact reason for this discrepancy remains unclear and may be related to the properties of the BODIPY fluorophore (Figs. 6c and d).

Several fluorescent probes mentioned above leverage the strong nucleophilic properties of alcohol hydroxyl groups, exhibiting high sensitivity and rapid response times. This characteristic also inspires the design of new fluorescent probes for nerve agents. In contrast, the phenolic hydroxyl group possesses relatively weak nucleophilic properties and is less prone to phosphorylation, resulting in lower sensitivity for phenolic hydroxyl group-based fluorescent probes in nerve agent detection. Nevertheless, thoughtful molecular design can significantly enhance effectively improve the sensitivity of these probes.

For instance, Kim and Lu reported two BODIPY-based fluorescent probes **11** and **12** [54,55]. Their drop-coated films exhibited significant fluorescence enhancement in response to DCP vapor, which allowed for the exclusion of interference from hydrochloric acid. Although both probes demonstrated similar fluorescence enhancements when exposed to DCNP, the corresponding response mechanisms were not explored in detail. In fact, the mechanisms for the response to DCP differ: For probe **11**, phosphorylation of the hydroxyl group inhibits the intramolecular rotation process, resulting in fluorescence enhancement. In contrast, the strong electron-withdrawing ability of the cyano group in probe **12** leads to a pronounced PET process, which can be interrupted by the phosphorylation of the hydroxyl group, thereby restoring the fluorescence of BODIPY. These results indicate that the sensing mechanisms differ significantly following various modifications to the BODIPY molecules, despite the similar fluorescence changes observed. Therefore, it is essential to further investigate relationship between the molecular structures and their corresponding re-

Table 1
Toxicological data of key OPNAs and OPFRs.

Probes	λex/λem (nm)	Mechanism	Switching type	Response time	LOD	Target	Application	Ref.
1	450/710	CT	Turn on	15 s	No data	DFP/DCP	Film	[46]
2	314/370	PET	Turn on	No data	No data	DFP/DCP	Solution	[47]
3	273/345	PET	Turn on	No data	No data	DFP/DCP	Solution	[47]
4	291/385	PET	Turn on	No data	No data	DFP/DCP	Solution	[47]
5	470/515	ICT	Turn on	72 s	5/3 ppm	DCNP/DFP	Paper	[50]
6	470/507	ICT	Turn on	122 s	7/8 ppm	DCNP/DFP	Paper	[50]
7	530/555	ICT	Turn on	No data	0.1/0.39 ppm	DCNP/DFP	Solution	[49]
8	530/575	ICT	Turn on	No data	4.01/6.10 ppm	DCNP/DFP	Solution	[49]
9	470/505	ICT	Turn on	No data	0.2/- ppm	DCNP/DFP	Film	[51]
10	395/440	PET	Turn on	No data	No data	DECP/DIFP	Film	[48]
11	502/522	PET	Turn on	15 s	No data	DCP	Paper	[54]
12	480/531	PET	Turn on	540 s	20.7 ppb	DCP	Paper	[55]
13	465/546	ICT	Ratio	No data	1.82 ppb	DCP	Paper	[56]
14	320/375	ICT	Ratio	No data	8 nmol/L	DCP	Film	[57]
15	365/418	ICT	Ratio	No data	No data	DCP	Film	[58]
16	365/550	HLCT	Turn off	No data	0.15 ppb	DCP	Paper	[42]
17	365/575	TADF	Turn off	5 s	2.5 ppb	DCP	Film	[59]
18	430/510	ESIPT	Turn on	No data	1.3 nmol/L	DECP	Fiber	[60]
19	580/593	PET	Turn on	2 min	No data	DCP	Film	[61]
20	365/540	ICT	Ratio	No data	4.0 ppm	DCP	Film	[62]
21	361/440	ICT	Turn off	No data	0.7 ppb	DCP	Paper	[63]
22	357/468	ICT	Turn off	3 s	65 ppt	DCP	Film	[64]
23	365/480	No data	Ratio	No data	6 ppm	DCP	Film	[65]
24	365/550	PET	Ratio	No data	0.1 nmol/L	DCNP	Film	[66]
25	365/553	HLCT	Turn off	2.1 s	21 ppt	DCP	CMP film	[67]
26	365/548	HLCT	Turn off	5 s	2.5 ppt	DCP	CMP film	[67]

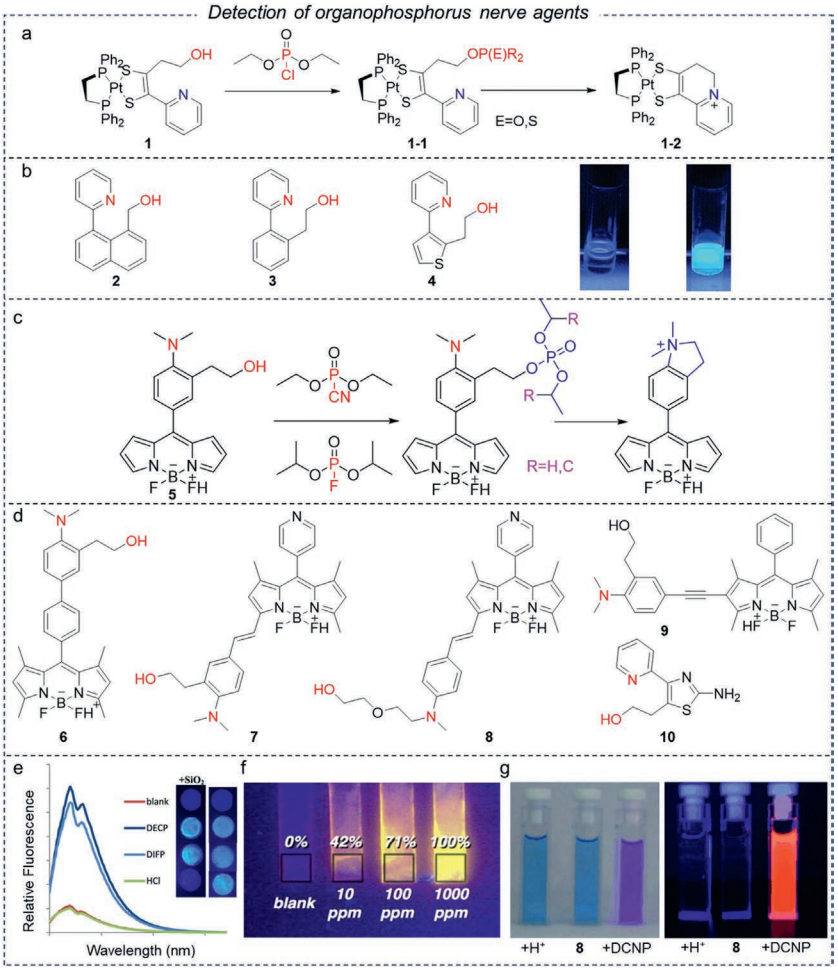


Fig. 6. (a) Schematic of the detection of probe **1**. (b) Structures of probes **2**-**4** and fluorescence changes in probe **2**. Reproduced with permission [47]. Copyright 2003, American Chemical Society. (c) Mechanism of the response of probe **5** to DCNP and DFP. (d) Chemical structures of probes **6**-**10**. (e) Fluorescence response of silica dispersed probe **10** films to hydrochloric acid was weakened. Reproduced with permission [48]. Copyright 2014, WILEY-VCH. (f) Probe **9** strips immersed in distilled water contaminated with 0, 10, 100, and 1000 ppm DCNP. Reproduced with permission [51]. Copyright 2014, Elsevier. (g) Visual changes observed for **8** in the presence of acid or DCNP. Reproduced with permission [49]. Copyright 2014, WILEY-VCH.

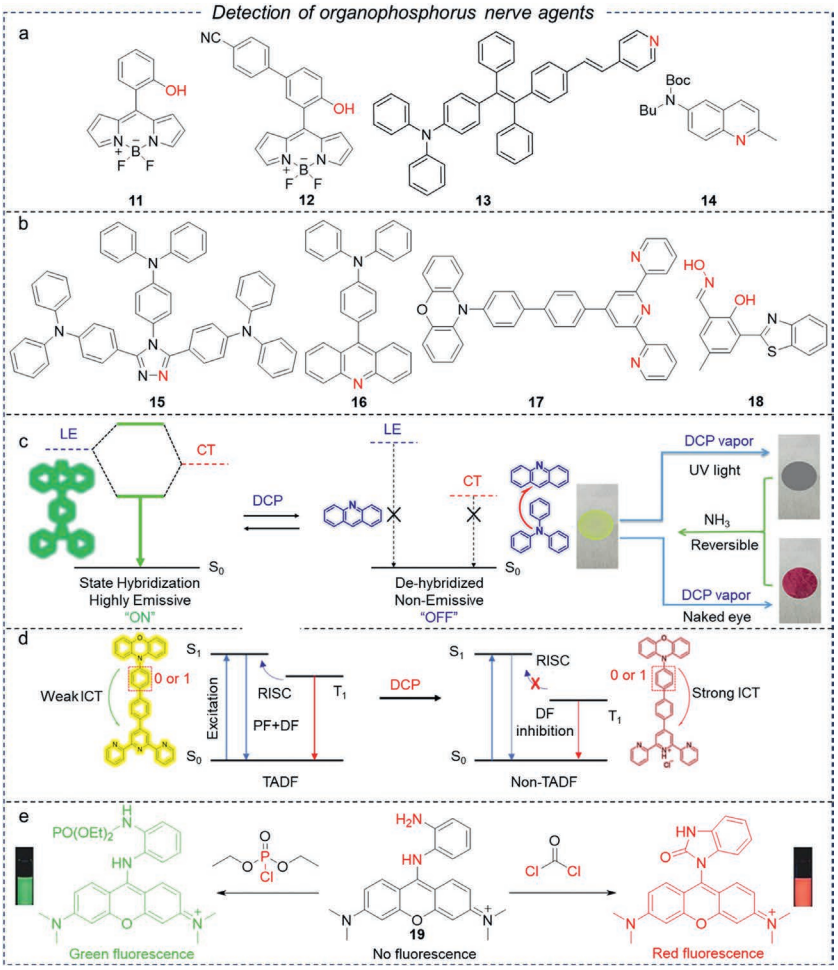


Fig. 7. (a) Schematic diagram of the structures of probes **11**-**14**. (b) Schematic diagram of the structures of probes **15**-**18**. (c) Recoverable fluorescence and color response of probe **16** test strips to DCP vapor based on the mechanism of DCP vapor detection by de-hybridized HLCT excited states. Reproduced with permission [42]. Copyright 2019, American Chemical Society. (d) Probe **17** TADF-based mechanism for detecting DCP. Reproduced with permission [59]. Copyright 2025, American Chemical Society. (e) Response mechanism of probe **19** to DCP. Reproduced with permission [61]. Copyright 2016, WILEY-VCH.

sponse mechanisms. Besides, while both probes demonstrated an acceptable fluorescence response to DCP, organic bases must be incorporated as additives into the films to accelerate the phosphorylation reaction, due to the weaker nucleophilicity of phenolics. This requirement may increase the overall cost of using the probes (Fig. 7a).

Among these compounds, small molecules that contain nitrogen-containing heterocycles exhibit strong nucleophilicity and good solubility, allowing for their rapid preparation into sensing films through various methods. They are most commonly employed in the gas-phase detection of nerve agent mimetics. Typical pyridine groups can efficiently catalyze the hydrolysis of DCP, resulting in the formation of pyridine salts that enhance the ICT effect of probe molecules, leading to a red shift in fluorescence emission.

Wu *et al.* simultaneously modified diphenylamine and pyridine on TPE to develop an aggregation-induced emission (AIE) probe **13** which exhibits ICT properties [56]. Probe **13**'s pyridine moiety, acting as both a recognition group and an electron acceptor. Its nucleophilic attack on the phosphonium ylide forms an unstable intermediate, whose N-P bond is susceptible to weak nucleophiles, leading to hydrolysis into pyridinium salts. The filter paper film emits bright yellow light and exhibits a gradual shift in fluorescence from yellow to orange as the concentration of DCP vapor varies. As a ratiometric probe that utilizes dual-emission variation, it facilitates robust detection by minimizing environmental interference.

For ICT-based probes, pH influences the charge distribution within the electron donor-acceptor system. Under acidic conditions, the protonation of the electron acceptor enhances ICT, resulting in redshifted emission even in the absence of OPs, which can interfere with specific detection. Therefore, pH-buffered systems are essential when employing these probes in complex matrices.

Molecular design strategies have been widely adopted, and various nitrogen-containing heterocyclic small molecules based on different ICT mechanisms have been reported by Song *et al.* [57]. The amine-supply capacity significantly influences the nucleophilicity of the pyridine atom, as it affects both the protonation ability and the ICT effect of the probes. In this context, probe **14** exhibits a rapid ratio metric fluorescence response (<100 s) to DCP, with LOD of 8 nmol/L. However, this probe is unable to clearly differentiate between acidic gases and DCP vapor. Moreover, Zhang *et al.* reported a triazole-based ICT molecule whose fluorescence emission from spin-coated films and test strips was rapidly red-shifted upon exposure to DCP vapor [58]. Importantly, reusable films enable multiple cycles of DCP detection with a response time of less than 1 s (Fig. 7b).

In addition to the aforementioned ICT mechanism, Ma *et al.* reported a hybrid excited state molecule, designated as probe **16**

[42]. This molecule features triphenylamine as the donor and acridine as the acceptor, resulting in an excited state characterized as a hybrid state (formed by the hybridization of local and charge transfer states). Upon exposure of the test strip to DCP vapor, the acridine group undergoes protonation, leading to the disappearance of the hybrid state property and the formation of a non-luminescent CT excited state which causes a quench of fluorescence. This marks the first application of HLCT fluorescent molecules in the fluorescence detection of DCP, thereby enriching the current understanding of excited state properties (Fig. 7c). Subsequently, Ma *et al.* utilized TADF fluorescent molecules for the first time in the fluorescence detection of DCP, further enhancing the existing knowledge of excited state properties (Fig. 7d, probe **17**) [59]. Meanwhile, current pyridine-based materials containing sp^2-hybridized nitrogen atoms can respond to both DCP and protonic acids simultaneously; however, they are unable to effectively distinguish between the two in practical environments. Consequently, the researchers selected SiO_2 as an acid buffer for the preparation of thin films and K_2CO_3 to inhibit the hydrolysis of DCP in natural settings.

Other N-containing small molecules, such as oximes that also possess hydroxyl groups, respond more rapidly to DCP than phenols. Yoon *et al.* developed probe **18**, which is based on the hydroxy benzothiazole fluorophore, salicylaldoxime, for the detection of DCNP [60]. The probe utilizes the ESIPT effect associated with keto- and enol-type transformations of hydroxy benzothiazole, and exhibits weak fluorescence in the absence of DCNP. Upon interaction with DCNP, the hydroxyl group in the probe undergoes phosphorylation, resulting in the formation of an electron-withdrawing nitrile group. This modification inhibits the ESIPT process of the probe, leading to a significant enhancement in fluorescence (>60-fold).

However, most oxime-containing small molecules can only be utilized under strongly alkaline conditions, which limits their practical significance. The mechanism for detecting DCP using amino-containing molecules is analogous to that of phenol; in this process, the amino group undergoes phosphorylation, inhibiting the PET process within the molecule and thereby restoring the emission of the fluorophore. Notably, probe **19** not only detects DCP but also selectively differentiates phosgene (an asphyxiating agent), making it the first fluorescent probe capable of responding to both DCP and phosgene while distinguishing between the two [61].

Conjugated polymers are fluorescent materials characterized by a structure that does not easily achieve a twisting angle comparable to that of small organic molecules [68]. This limitation results in a significant spectral shift during sensing applications. In contrast to small molecule fluorescent groups, conjugated polymers and oligomers not only exhibit fluorescent activity but also demonstrate a "molecular wire effect". Because their main chains function as molecular pathways, enabling excitons to propagate rapidly throughout the entire polymer chain and resulting in exceptionally high exciton mobility. Organic small molecules adhere strictly to stoichiometric ratios when interacting with analytes [69]. In contrast, when a repeating unit of a conjugated polymer interacts with an analyte molecule, the resulting fluorescence quenching diffuses throughout the polymer chain. This diffusion leads to a rapid change in fluorescence across the entire polymer in a very short period of time. Meanwhile, the amplified sensing phenomenon is influenced by factors such as the lifetime and migration rate of excitons.

There is a lack of research addressing the use of fluorescent polymers in the field of vapor detection for nerve agent mimetics. Most reported polymer fluorescent probes utilize nitrogen heterocycles as electron acceptors and recognition groups. Lee *et al*. synthesized probe **20**, a quinoxaline-based main-chain conjugated polymer. The fluorescence of the dip-coated film was rapidly quenched upon exposure to DCP, and the fluorescence emission intensity was restored by treatment with an aqueous solution of NaOH, thereby enabling the development of a reversible paper-based sensor (Figs. 8a and c) [62]. Recently, Zhang *et al*. developed a fluorescent conjugated polymer probe **21** with a weak ICT effect for the detection of DCP [63]. Upon the addition of DCP, the N on TAZ attacks the phosphoryl chloride of DCP, forming an unstable adduct. This intermediate rapidly hydrolyzes, resulting in removal of the unstable leaving group and partial decomposition into a hydrochloride compound through two phosphorylation processes, ultimately achieving protolysis. The ICT effect of probe **21** was enhanced, and the fluorescence probe exhibited an instantaneous red-shift in fluorescence (440 nm-500 nm), with a LOD of 2.3 nmol/L in solution (Figs. 8a and d).

Cheng *et al.* designed probe **22** with a pyrene core linked by a fluorene unit to tripyridine sensing unit for DCP detection [64]. Under the influence of the electron pair from the pyridine unit, pyridinium phosphate can form in the presence of electrophilic DCP, subsequently undergoing a hydrolysis reaction that produces pyridinium hydrochloride and enhances the ICT effect. The emission peak of the probe red-shifted from 468 nm to 554 nm. The fluorescence of probe **22** in the as-prepared spin-coated film was completely quenched in DCP saturated vapors within 3 s, with a fluorescence quenching rate of 3.6% for 65 ppt of DCP (Fig. 8b). Swager *et al*. discovered that ethanolated chains in polymerized chromophores, such as tetraethylene glycol monomethyl ether, can achieve colorimetric responses to DCP vapors at LOD of 6 ppm. In contrast, the non-ethanolated polymers in the film exhibited no detectable color change, even when exposed to saturated DCP vapor. The presence of ethanolated chains may enhance the diffusion of DCP into these polymers, thereby increasing the colorimetric response. Additionally, the increased polarity and flexibility of the ethanolated chains may facilitate rapid reactions between the hydroxyl groups and DCP in the sensing material. (probe **23**) This demonstrates that highly sensitive detection of OPNAs can be achieved through the strategic use of thin film structures and matrix effects [65].

Lee *et al.* proposed a polymer fluorescent probe **24** for the selective detection of DCNP in both solution and vapor states, utilizing glycidyl methacrylate and dimethylacrylamide [66]. In this probe, DCNP induces *N*-alkylation, biophosphorylation, and intramolecular cyclization within the molecule. These processes limit the PET effect and lead to enhanced fluorescence of the probe, which exhibits a distinct color change from purple to colorless, with a 1.0 mmol/L LOD (Fig. 8e).

Recently, Ma *et al*. proposed a sensor design based on a conjugated microporous polymer (CMP) film [67], which has revolutionized on-site detection by integrating materials engineering with sensing mechanisms. This CMP film synergizes three key features: HLCT/de-HLCT state switching, microporous structures for rapid gas diffusion, and conjugated backbones for signal amplification. As a result, it enables detection of DCP at levels as low as 1.7 ppt, setting a new benchmark for ultra-trace vapor sensing (Fig. 8f).

3.4. Pesticides

Organophosphorus pesticides (OPPs) are a major class of agrochemicals used worldwide to control insects, mites and other arthropod pests. They function by inhibiting AChE in target organisms, rapidly disrupting neural transmission and causing mortality. Functional groups in the molecules of OPPs or their hydrolysis and reduction products, such as AchE or organophosphorus hydrolases (OPH) [70,71], can chemically react with specific reagents. When these compounds are irradiated with a specific wavelength of excitation light, they emit light at a particular wavelength, enabling di-

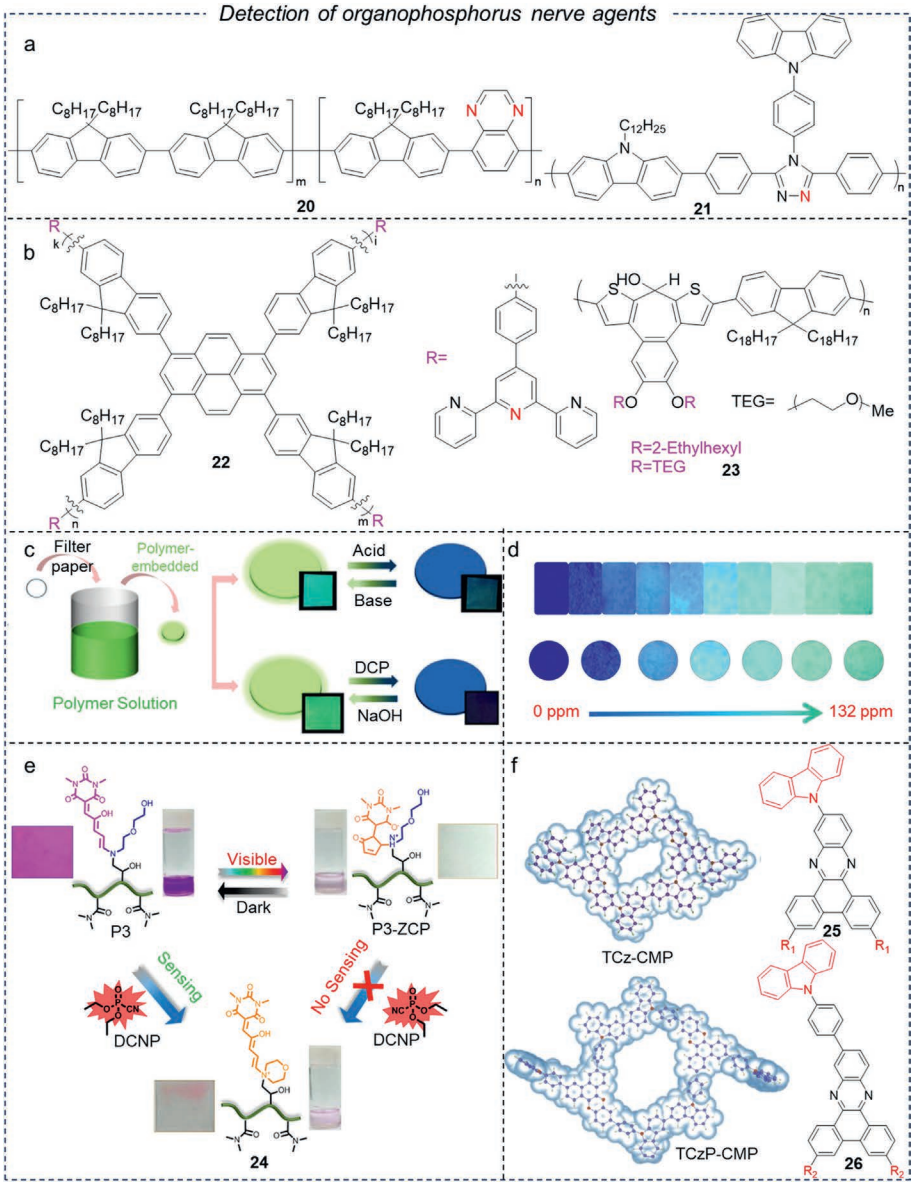


Fig. 8. (a) Schematic diagram of the structures of probes **20** and **21**. (b) Schematic diagram of the structures of probes **22** and **23**. (c) Schematic of acid-base switching and DCP sensing using paper-based probe **20**. Reproduced with permission [62]. Copyright 2014, American Chemical Society. (d) Fluorescence changes of probe **21** exposed to DCP vapor at different concentrations. Reproduced with permission [63]. Copyright 2020, Elsevier. (e) Schematic of visible light responsive probe **24** switching for switching colorimetric detection of nerve agent simulants. Reproduced with permission [66]. Copyright 2016, American Chemical Society. (f) The optimal configuration of probes **25** and **26** calculated by TD-DFT. Reproduced with permission [67]. Copyright 2022, Springer Nature.

rect quantitative detection. Furthermore, the characteristic groups in the OPPs can interact with the probe's active site through either nucleophilic substitution or chelation reactions [72].

In recent years, polymer fluorescent probes have shown great potential in the field of OPPs detection due to their customizable structural design, signal amplification capabilities, and environmental stability. Porous organic polymers, and water-soluble fluorescent polymers have been developed for a wide range of applications. Based on the irreversible inhibitory effect of OPPs on AChE activity, Liu *et al.* inhibited the hydrolysis of ATCh to produce acetic acid, which affected the pH of the solution and diminished the protonation of the fluorescent probe **27** [73], which contains aldehyde and tetraphenylethene (TPE) derivatives. This process established a signal for the fluorescence detection of DMT (Fig. 9a). Similarly, Wang *et al.* determined the concentrations of OPPs by utilizing the pH changes that occur during the reaction between AChE and OPPs. Using this strategy, they designed fluorescent probe **28** to detect malathion and parathion in fruit juice samples (Fig. 9b) [74].

Although the detection methods mentioned above exhibit high sensitivity, they lack selectivity and are unable to differentiate acid interference in certain complex environments. Consequently, researchers have substituted the analyte derived from hydrolysis products with enzymes, leading to significant advancements in the sensitive and direct identification of esterases through the use of enzyme-activated small molecule fluorescent probes. Li *et al.* proposed probe **29** based on the AIE effect of TPE and the addition reaction ability of maleimide groups [75]. During the detection process, the electrophilic reaction between TPE and AChE catalyzed hydrolysis products was employed to generate molecules with strong fluorescence *in situ* (Fig. 9c). The fluorescence intensity of these molecules is dependent on the activity of AChE or the concentration of Diazinon. To prevent interference from IFE in real sample matrices, Lu *et al.* developed an AChE-activated near-

Table 2
Summary and comparison of published fluorescent probes for pesticides.

Probes	λex/λem (nm)	Mechanism	Switching type	Response time	LOD	Target	Application	Ref.
27	365/446	ICT	Turn on	No data	0.008 mg/L	DMT	Water	[73]
28	290/330	ICT	Turn off	No data	0.16 μg/L, 0.24 μg/L	Malathion, DMT	Fruit juices	[74]
29	365/465	AIE	Turn off	180 s	0.23 ng/L	Diazinon	Serum	[75]
30	660/700	CT	Turn on	No data	0.0186 μg/L, 12.3 μg/L	DDVP, CPF	Food	[76]
31	385/445	ICT	Ratio	No data	2.49 ng/mL	Paraoxon	Food, Cell	[77]
32	365/478	CT	Turn off	No data	No data	GLYP	Water	[81]
33	365/478	CT	Turn off	No data	No data	GLYP	Water	[82]
34	365/500	AIE	Turn on	15 min	0.6 μmol/L	EP, MP	Food	[79]
35	380/475	IFE	Turn on	No data	0.49 nmol/L	CPF	Water	[80]

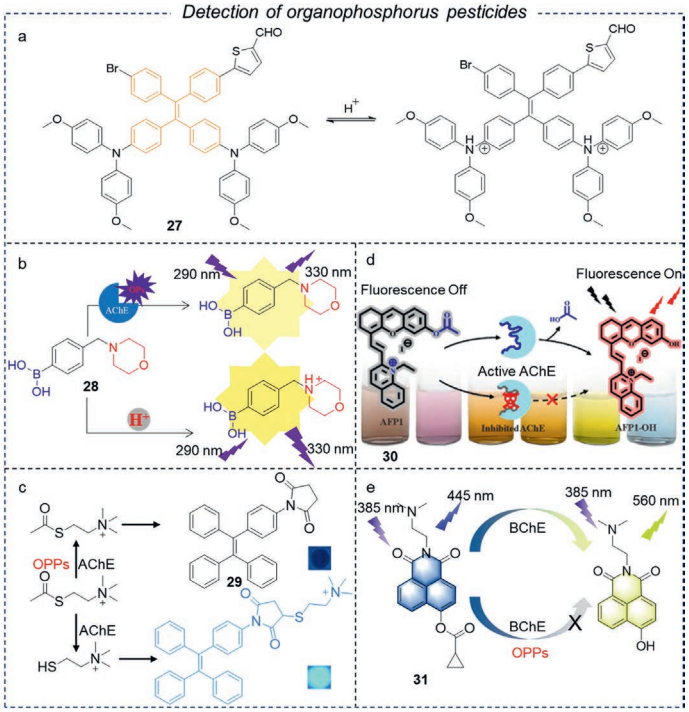


Fig. 9. (a) Proposed pH sensing mechanism using probe **27**. Reproduced with permission [73]. Copyright 2019, Elsevier. (b) Schematic illustration of the detection mechanism of probe **28**. Reproduced with permission [74]. Copyright 2021, Elsevier. (c) Schematic illustration of the detection principle of probe **29** for AChE activity and Diazinon. Reproduced with permission [75]. Copyright 2016, Elsevier. (d) Anti-interference sensing of OPPs and CM pesticides with probe **30** in colored samples. Reproduced with permission [76]. Copyright 2023, Elsevier. (e) Graphical representation of the response mechanism of probe **31** to BChE and OPPs. Reproduced with permission [77]. Copyright 2025, Elsevier.

infrared (NIR) fluorescent probe for the anti-interference measurement of OPPs and CM pesticides in colored samples (Fig. 9d) [76].

Currently, researchers are focusing on butyrylcholinesterase (BChE), which exhibits a greater responsiveness to OPPs, and Nie *et al.* have developed a dual-wavelength probe **31** utilizing the ICT mechanism [77]. This innovative design mitigates the issues of photobleaching and environmental interference with conventional single-wavelength probes [78], resulting in enhanced accuracy and sensitivity for the detection of OPPs (Fig. 9e).

In addition to small molecular fluorescent probes, porous organic polymers (POPs) have emerged as a significant focus of interest in the field of OPPs fluorescence sensing in recent years due to their distinctive high specific surface area and tunable pore structures (Table 2). Wang *et al.* reported for the first time the use of fluorescent probe **32** for the detection of toxic pesticides, utilizing fluorescent porous organic polymers as probes (Fig. 10a). They synthesized fluorescent microporous and mesoporous polyamides containing trityl amine chromophore groups, which enabled the detection of a broad range of OPPs [81]. Energy transfer between the electron-rich triphenylamine and the electron-deficient fluroxypyr was more efficient than that with fenitrothion and glyphosate. Additionally, they designed a new porous polymer probe **33** that enhances the flexibility of the carbazole chromophore (Fig. 10b), allowing for more efficient energy transfer from the carbazole moiety to neighboring pesticide molecules [82]. The sensitivity of chemical sensing was improved by optimizing the fluorescence and porous characteristics of the polymer.

Wang *et al.* developed a biomimetic fluorescent TPE peptide probe **34** for detecting MPs and EPs by binding AIE molecules to the amino acid site of an alternating hydrophilic and hydrophobic peptide component, as well as to catalytic triads containing serine (Fig. 10c). The formation of a covalent bond between the probe and the OPPs increases the probe's hydrophobicity, facilitates its aggregation, and enhances the fluorescence emission of the TPE [79]. Vandana Bhalla *et al.* developed a metal-free fluorescent supramolecular probe **35**, based on anthracene/perylene bisamide (PBI) derivatives. This probe was utilized to detect chlorpyrifos by forming tightly packed assemblies with CPF [80]. Solvent polarity and miscibility influence the interactions between probes and OPs through molecular conformation, reaction kinetics, and photophysical properties [83]. In the case of AIE-active probes, solvent hydrophobicity plays a crucial role in driving aggregation. Nonpolar solvents may induce pre-aggregation of probes, leading to false positive results.

3.5. Flame retardants

Organophosphorus flame retardants (OPFRs) are a class of additive or reactive chemicals that inhibit or delay the combustion of polymeric materials by promoting char formation, quenching free radicals in the gas phase, or both. Widely employed in plastics, textiles, foams and electronic housings, they offer an alternative to halogenated flame retardants by combining effective fire performance with reduced release of halogenated dioxins and furans during combustion [84]. During manufacturing, service life and end-of-life stages, OPFRs can migrate out of polymer matrices into surrounding air, dust and wastewater due to their relatively low molecular weight and moderate polymer affinity. Once released, they resist rapid biodegradation and exhibit varying degrees of water solubility and lipophilicity, leading to persistent environmental dispersion [85]. OPFRs have been detected in indoor dust, surface waters, sediments and biota, where they may bioaccumulate and exert endocrine-disrupting or neurotoxic effects. This ubiquitous leaching and persistence transform beneficial flame retardants into pervasive OPs pollutants, raising concerns over long-term human and ecological exposure [86]. The environmental residues and biological toxicity of these substances are often underestimated due to a lack of targeted testing techniques. In recent years, organic fluorescent probes for OPFRs have gradually emerged. However, there

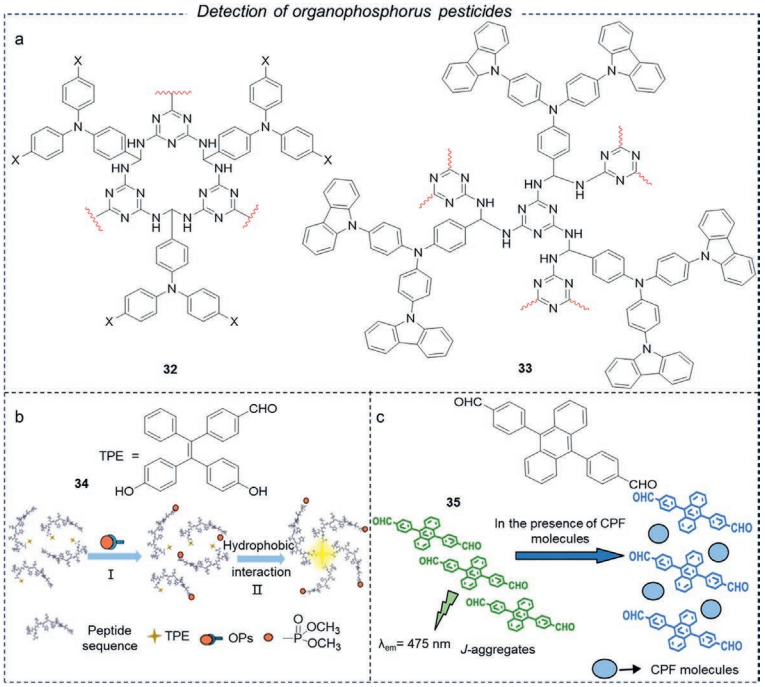


Fig. 10. (a) Monomer structure of polymer fluorescent probes **32** and **33**. (b) Schematic diagram illustrating the operating principle of probe **34**. Reproduced with permission [79]. Copyright 2020, Elsevier. (c) Schematic representation of the assemblies of probe **35** in the presence of CPF and the TEM image in solution. Reproduced with permission [80]. Copyright 2020, Elsevier.

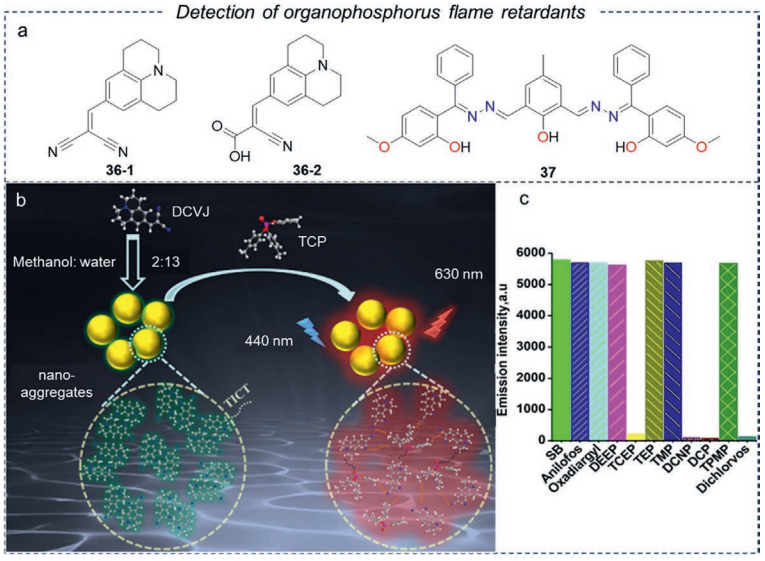


Fig. 11. (a) Schematic diagram of the structure of probes **36** and **37**. (b) The proposed mechanism of the influence of the interaction between probe **36-1** and TCP on fluorescent intensity. Reproduced with permission [90]. Copyright 2024, Elsevier. (c) A comparison of emission intensity of probe **37** at 533 nm in the presence of different organophosphates showing selectivity for TCEP, DCNP, DCP and DDVP. Reproduced with permission [91]. Copyright 2020 Elsevier.

are limited organic fluorescent probes available for the detection of flame retardants.

Gong *et al.* improved the chemiluminescent signal for the detection of TCEP using the classical luminol- H_2O_2 system [87]. Subsequently, they proposed an indirect method for determining trace amounts of TPHP based on HPA-luminol chemiluminescence enhancement [88]. They also developed the first fluorescence probe for TCP [89]. During the same period, they introduced a fluorescent probe for detecting TCP, utilizing the commercial compound 9-(2,2-dicyanovinyl)-julotine (DCVJ) as fluorescent probe **36-1** (Fig. 11a) [90]. Due to the TICT state, the DCVJ probe exhibits significant aggregation-induced emission (AIE) properties compared to probe **36-2**. The fluorescence response mechanism indicates that hydrophobic interactions and conjugation effects between TCP and DCVJ restrict the rotation and vibration of the DCVJ molecule, thereby triggering the fluorescence. This study offers new insights for the efficient detection of emerging OPFRs contaminants (Fig. 11b).

Kaur *et al.* designed and synthesized a stilbene-based Schiff base for the detection of TCEP and OPPs [91]. The probe exhibited quenching in the presence of organophosphates due to the formation of covalent bonds between the OPs pollutants and the -OH group on the probe. Interestingly, the sensing probe can degrade toxic OPs compounds in the presence of Zn^{2+}, demonstrat-

Table 3
Summary and comparison of published fluorescent probes for flame retardants.

Probes	λex/λem (nm)	Mechanism	Switching type	Response time	LOD	Target	Application	Ref.
36	440/510	TICT	Ratio	No data	4.82 ng/mL	TCP	Water	[90]
37	420/533	ESIPT	Ratio	No data	122.7 nmol/L	TCEP	Soil	[91]

ing its potential as a bifunctional material for both the detection and degradation of OPs compounds (Fig. 11c).

The development of organic fluorescent probes for the detection of OPFRs is currently underway (Table 3). The primary challenges at this stage include the following: due to the structural similarities between OPFRs and other OPs, it may be difficult for probes to achieve specific identification of the target may prove difficult for the probes. Additionally, a wide range of interfering substances present in the environment can adversely effect on the accuracy of the fluorescence signals. Furthermore, the recycling and subsequent treatment of the probes have emerged as urgent issues that must be addressed prevent secondary environmental pollution.

4. Perspective on characterizing new fluorescent probes

As previously mentioned, numerous fluorescent probes have been developed for the detection of OPs pollutants. However, these fluorescent probes still face several challenges, including low sensitivity and instability when exposed to light and heat. Researchers are actively investigating fluorescent probes with higher sensitivity and improved stability to meet practical application requirements. Over the past five years, this trend has significantly accelerated the synthesis of novel fluorescent probes with superior optical properties. Nevertheless, many of these fluorescent materials remain at the stage of theoretical prediction rather than undergoing further experimental validation. Fortunately, current efforts are focused on comprehensively assessing the performance of novel fluorescent sensing materials from both computational and experimental perspectives. To achieve this goal, we aim to provide a more accurate evaluation of the performance of innovative fluorescent probes through newly proposed characterization methods, thereby advancing research in this field.

4.1. Theoretical calculations

Quantum chemical calculations serve as powerful tools for studying the electronic structures of molecules, providing valuable predictions and analyses of the optical properties of fluorescent probes. Among these methods, density-functional theory (DFT) has been widely utilized to calculate the electronic structure of certain molecules in their ground state. Specifically, information such as energy levels and electron density distributions can be obtained using this method. Time-dependent density-functional theory (TD-DFT) is an extension of DFT that is additionally employed to calculate the excited state properties of molecules, including absorption and emission spectra associated with electron transitions [92]. In combination, DFT and TD-DFT allow for an accurate description of the excited state and optical properties of molecules, offering improved predictions and explanations of the optical characteristics of molecules and materials at a low computational cost in the fields of quantum chemistry and molecular physics [93,94]. By performing TD-DFT calculations, the widely used quantum chemistry program Gaussian is required for molecular structure optimization and energy level calculations, followed by calculations of excited state structures and spectral properties. Notably, the most stable molecular structure is achieved by selecting an appropriate basis set along with density functions and performing geometrical configuration optimization calculations. Next, energy level calculations are performed on the optimized molecular structures, yielding the ground and excited state energy levels of the molecule are obtained from the calculations. Finally, based on these energy levels, the absorption and fluorescence spectra of the molecules are attained, as the calculated spectra are achievable to analyses the absorption and emission properties of the molecules in each excited state. In addition to the calculation of molecular structures and energy levels, several other factors must be considered under TD-DFT calculation. The first factor involves selecting appropriate basis functions and density generalization, which directly affect the accuracy and reliability of the calculation results. The second factor considered is the solvation effects, as well as the influence of environmental factors on the optical properties of the molecules. These can be addressed by incorporating a suitable solvent model into the calculations, which extends the capabilities of TD-DFT [95,96]. Finally, certain issues related to accidents, such as computational errors and numerical stability, must be addressed, particularly concerning the TD-DFT method. Due to the time-dependent nature of excited state wave functions, it is essential to ensure computational stability to obtain accurate excited state and spectral properties.

Jacquemin *et al*. provides valuable insights on this topic [97]. For instance, theoretical calculations play a crucial role in the research and development of fluorescent probes, enabling researchers to predict their performance and offering innovative guidance for pre-synthesis and enhancement. However, it is important to note that the results of theoretical calculations must be validated through experiments, as experimental conditions and the behavior of molecules in complex environments can significantly influence the actual performance of fluorescent probes. In summary, both theoretical calculations and experimental studies should be encouraged to advance fluorescent probe technology.

4.2. Optical characteristics

It is undeniable that fluorescence detection relies on optical signals to gather information. Therefore, the optical properties of fluorescent probes are crucial for their practical applications, which are primarily determined by the following aspects: absorption spectra, emission spectra, photostability, fluorescence lifetime, quantum yield, selectivity, specificity, and environmental sensitivity (Fig. 12). Indeed, these characteristics offer significant guidance in the design of effective probes.

Among them, absorption and emission spectra are two fundamentals for the characterization of the optical properties, which are essential for deeply understanding or effectively applying them into design of fluorescent probes. The absorption spectrum is obtained using UV–vis spectroscopy, which measures the distribution of absorbed light energy by a substance when irradiated at different wavelengths. This spectrum reflects the light-absorption energy and is typically used to determine the maximum absorption wavelength (λ_{max}) of the molecule. During the testing process, it is crucial to select a solvent that offers good solubility and selectivity for the sample, ensuring that there is no light absorption within the measured spectral range to avoid interference with the results. Additionally, the sample concentration should be moderate to prevent absorption saturation, which can occur at high concentrations, or undetectable absorption at low concentrations. The transparent surface of the cuvette should be cleaned with lens paper from top to bottom, and attention should be paid to the pairing of cuvettes.

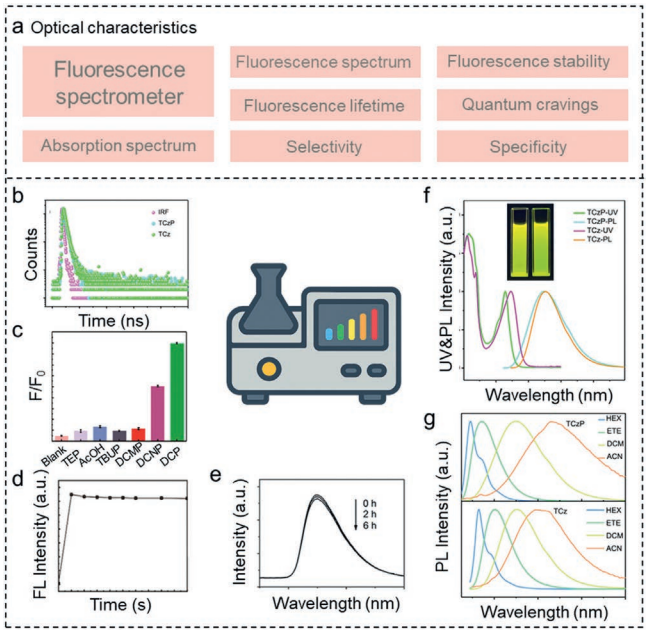


Fig. 12. (a) Characterization of the optical properties of fluorescent probes. (b, f, g) Reproduced with permission [67]. Copyright 2022, Nature. (c, d) Reproduced with permission [98]. Copyright 2023, American Chemical Society. (e) Reproduced with permission [99]. Copyright 2021, Wiley-VCH.

The solution in the cuvette should fill approximately 2/3 to 4/5 of its height [100].

On the other hand, the emission spectrum refers to the distribution of light emitted from a substance after it absorbs light at a specific wavelength. Measurements of this spectrum are commonly conducted using a fluorescence spectrometer. The emission spectrum reflects the characteristics of the light emitted from the substance upon excitation, including the maximum emission wavelength of fluorescence. First, the sample is excited to the level of light-absorption energy, after which the intensity and wavelength distribution of the emitted light are accurately recorded. To obtain the strongest emission signal, the maximum absorption wavelength is typically chosen as the appropriate excitation wavelength based on the sample's absorption spectrum. This is important because prolonged exposure to light may lead to photobleaching of the sample, significantly affecting the stability of the emission spectrum; therefore, the duration of the measurement should be carefully adjusted. Additionally, environmental factors such as pH and solvent type can influence both the UV absorption and emission spectra, so experiments should be conducted under controlled conditions [101]. Overall, precise measurements of the absorption and emission spectra are crucial for investigating the optical properties of a new fluorescent probe. Experimental conditions must be meticulously controlled, and attention should be given to the accuracy and repeatability of the data during the characterization process [102].

Following the developments in fluorescent materials, photobleaching has emerged as a significant limiting factor that causes attenuation of fluorescence intensity. Commonly, photobleaching process refers to the loss of energy from fluorescent molecules through non-radiative pathways after they absorb light energy. This energy loss can occur due to collisions with solvent molecules, conversion to thermal energy, or photochemical reactions, ultimately resulting in the loss of fluorescence [103]. Although the mechanism is not yet fully clarified for photobleaching yet, where the interaction occurred with molecular oxygen are considered one of the primary reasons. To minimize the negative effects of photobleaching, anti-bleaching agents are commonly employed, such as reactive oxygen scavengers, or by reducing the extent of triplet state formation to decrease the likelihood of molecular reactions with oxygen. Although it is essential to select fluorophores with strong photostability for fluorescence detection, there is currently no effective strategy to accurately predict the photostability of probes. This is because fluorophore extension and flexibility are often associated with lower photostability within the same compound family.

Fluorescence lifetime and fluorescence quantum yield describe a molecule's average lifetime in the excited state and its fluorescence efficiency, respectively. Accurate characterization of these two parameters is crucial for assessing the performance of fluorescent probes. Specifically, fluorescence lifetime refers to the time required time decreasing to 1/e of its maximum fluorescence intensity I_0 for a molecule after the excitation light is removed. During excitation by a laser beam, the molecule typically absorbs energy from the ground state to reach a certain excited state under excitation by laser beam, then emitting fluorescence as it returns to the ground state through a radiative transition. The fluorescence quantum yield refers to the probability of non-radiative decay during the fluorescence emission process, reflecting the luminescence efficiency of the fluorescent dye. It is defined as the ratio of the fluorescence emission intensity to the absorbed light intensity [104]. Generally, the value of the fluorescence quantum yield ranges between 0 and 1, with higher fluorescence emission efficiency indicated by values closer to 1. In detection, the size of the slit is crucial for fluorescence intensity, as enlarged slit can significantly increase both fluorescence intensity and reproducibility, although it may decrease resolution. Fluorophores with low quantum yield, such as CT-state emitters, require structural engineering techniques, such as HLCT hybridization in probe **16** [42] to enhance emission efficiency.

Additionally, the Stokes shift, the wavelength difference between absorption and emission maxima, minimizes self-absorption and IFE. ESIPT probes, such as probe **18** [60], and AIE probes, such as probe **34** [79] excel in complex matrices due to their significant shifts, ensuring robust signal differentiation. Besides, binding affinity quantifies the interactions of probes, directly influencing detection limits. High binding affinity values in pyridine-functionalized polymers, such as probe **22** [64] enable selective binding, achieving LODs as low as 65 ppt for DCP. Conversely, weak affinity, as seen in probe **11** [54], necessitates the use of additives to accelerate phosphorylation, complicating practical applications.

The practical application of fluorescent probes primarily depends on their selectivity and specificity. Selectivity refers to the probe's ability to distinguish between target and non-target molecules, while specificity indicates the probe's unique fluorescence response to the target molecule. For the selectivity of probes, it can be evaluated by measuring variations in fluorescence intensity in the presence of target and non-target molecules using fluorescence spectroscopy. In contrast, specificity can be assessed by observing changes in the emission spectra of the probe before and after the addition of the target molecule. Furthermore, introducing competitive substances can also help evaluate the probe's selectivity and specificity toward specific targets. However, it is crucial to ensure that only one variable is altered during the testing process to provide an accurate assessment of selectivity.

Overall, based on these experiments and studies, detailed information regarding the optical properties of fluorescent probes can be obtained and provide valuable design guidelines for customizing these probes to meet specific application requirements. The findings from this research are highly beneficial for the optical engineering of fluorescent sensing materials and for tailoring fluorescent probes with particular functionalities.

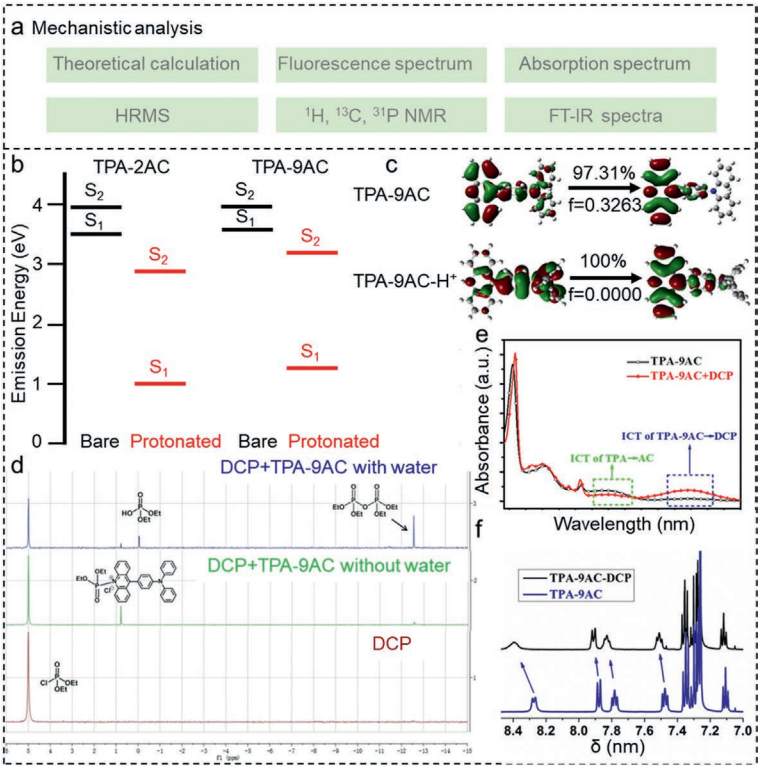


Fig. 13. Mechanistic analysis of fluorescent probes. Reproduced with permission [42]. Copyright 2019, American Chemical Society.

4.3. Mechanistic analysis

The detection mechanisms of fluorescent probes can be thoroughly analyzed and studied using various methods. Firstly, the detection mechanism of fluorescent probes can be examined using fluorescence spectroscopy analysis, measuring fluorescence intensity and emission peaks at different wavelengths. This approach provides valuable insights into the fluorescence properties and states of the probes. Additionally, examining the relationship between fluorescence and absorption spectra allows for the determination of the excitation light source for the fluorescent probes, as well as the wavelengths of the emitted fluorescence signals can also be determined, while preliminary inference can be made for the interaction mechanisms between fluorescent probes and their target molecules can also be made based on the changes observed in both fluorescence and UV absorption spectra.

A detailed evaluation of fluorescent-probe detection mechanisms requires both structural and reactive analyses. Infrared spectroscopy, nuclear magnetic resonance (NMR) and high-resolution mass spectrometry (HRMS) can characterize probe conformations and monitor functional-group transformations upon target binding [105]. Correlating these data with photophysical measurements (*e.g.,* shifts in absorption or emission) yields a mechanistic map of probe–analyte interactions. Such an integrated approach not only deepens our understanding of sensing pathways (Fig. 13) but also informs the rational optimization and design of next-generation probes for enhanced performance in real-world applications [93].

5. Conclusion and outlook

In this review, we have summarized recent advances in organic fluorescent probes for OPs pollutant detection, with particular emphasis on compound classification, toxicity profiles, and modes of poisoning. Small-molecule and polymeric probes exhibit complementary strengths for nerve agent identification, while porous organic polymers offer tailored binding sites ideally suited to pesticide recognition. Advances in flame-retardant sensing have been made, yet challenges in selectivity, interference suppression, and probe recyclability remain. To achieve the rational design of next-generation probes, we propose an integrated characterization framework comprising: (1) Quantum-chemical modelling of absorption and emission properties, (2) systematic evaluation of photophysical performance, and (3) mechanistic dissection of sensing pathways.

Current research on organic fluorescent probes encounters three significant challenges. First, issues related to the scalability and cost-effectiveness of synthetic routes are particularly evident in the difficulties associated with mass-producing BODIPY-based probes and the complex polymerization processes required for conjugated polymer probes. Second, false positives arise from insufficient selectivity, as some probes exhibit cross-reactivity with environmental interferents. For instance, the fluorescence responses of certain ICT-based and ESIPT-based probes can be influenced by pH variations in complex matrices, leading to inaccuracies. Third, the practical applicability of these probes in real-world environmental or biological samples is limited due to matrix interference. This interference can stem from substances such as humic acids or ions that quench fluorescence. Future efforts in OPs pollutant sensing could consider the following aspects: (1) The structure–property, particularly regarding the influence of electronic properties, recognition regions, and the regulation of organic probes on sensing performance. (2) Design probes capable of discriminating target analytes in complex matrices (*e.g.*, soil, blood) by minimizing cross-reactivity and matrix interference. (3) Develop arrays of complementary fluorescent probes where each responsive to distinct OP classes, to enable simultaneous identification and quantification of multiple pollutants. (4) Engineer cyclic or otherwise stabilized probe systems and validate their long-term

storage stability and performance under extreme environmental conditions. (5) Create NIR-emissive probes with proven biocompatibility for real-time, *in vivo* monitoring of OP exposure in animal models. (6) Integrate detection with catalytic or degradative functionality in a single probe to facilitate rapid pollutant identification alongside *in situ* detoxification. (7) Integrating fluorescent probes with Internet of Things technologies could create closed-loop systems in which unmanned aerial vehicles identify OPs contamination, smartphones validate on-site concentrations, and data are aggregated through cloud platforms to inform remediation efforts, thereby enhancing environmental and human safety.

Declaration of competing interest

The authors declare that they have no known competing financial interests or personal relationships that could have appeared to influence the work reported in this paper.

CRediT authorship contribution statement

Kun Song: Writing – review & editing, Writing – original draft, Visualization, Investigation, Formal analysis, Conceptualization. **Lijia Zhang:** Writing – review & editing, Writing – original draft, Formal analysis, Data curation, Conceptualization. **Yunhui Meng:** Writing – review & editing, Investigation. **Jiantong Ding:** Writing – review & editing, Visualization, Investigation. **Xiaobai Li:** Writing – review & editing, Validation, Supervision, Resources, Funding acquisition. **Yongpeng Liu:** Writing – review & editing, Visualization, Validation, Supervision, Project administration. **Hongwei Ma:** Writing – review & editing, Validation, Supervision, Project administration, Funding acquisition.

Acknowledgments

We are grateful for the financial supported by the National Natural Science Foundation of China (Nos. 22374017 and 22576031), Fundamental Research Funds for the Central Universities (No. 2572023CT12), the Natural Science Foundation of Heilongjiang Province (No. YQ2024B003).

Supplementary materials

Supplementary material associated with this article can be found, in the online version, at doi:10.1016/j.cclet.2025.111902.

References

[1] Z. Wei, H. Li, J. Wu, et al., Chin. Chem. Lett. 31 (2020) 177–180.
[2] K.M. Fahy, S. Lee, I. Akpinar, et al., J. Am. Chem. Soc. 146 (2024) 5661–5668.
[3] X. Hong, L. Yuan, X. Zhao, et al., Environ. Sci. Technol. 58 (2024) 13648–13657.
[4] Z. Xie, P. Wang, X. Wang, et al., Nat. Rev. Earth Environ. 3 (2022) 309–322.
[5] L. Zhang, K. Song, G. Liu, et al., Coord. Chem. Rev. 540 (2025) 216766.
[6] L. Jiang, M.M. Hassan, S. Ali, et al., Trends Food Sci. Technol. 112 (2021) 225–240.
[7] B.K. Singh, Nat. Rev. Microbiol. 7 (2009) 156–164.
[8] W.Q. Meng, A.C. Sedgwick, N. Kwon, et al., Chem. Soc. Rev. 52 (2023) 601–662.
[9] V. Kumar, H. Kim, B. Pandey, et al., Chem. Soc. Rev. 52 (2023) 663–704.
[10] Y. Zhao, Y. Fan, J. Li, et al., Environ. Sci. Technol. 58 (2024) 3332–3341.
[11] R.J. Drout, S. Kato, H. Chen, et al., J. Am. Chem. Soc. 142 (2020) 12357–12366.
[12] Y. Yang, H. Li, D. Liu, et al., Coord. Chem. Rev. 543 (2025) 216905.
[13] S. Tang, Z. Luo, J. Liao, et al., Chin. Chem. Lett. 34 (2023) 108090.
[14] M. Konieczny, G. Sosnovsky, Chem. Rev. 81 (1981) 49–77.
[15] P. Huang, W. Wu, M. Li, et al., Coord. Chem. Rev. 501 (2024) 215534.
[16] G.K. Sidhu, S. Singh, V. Kumar, et al., Crit. Rev. Environ. Sci. Technol. 49 (2019) 1135–1187.
[17] Y. Liu, L. Guo, P. Jin, et al., TrAC Trends Anal. Chem. 178 (2024) 117828.
[18] L. Chen, D. Wu, J. Yoon, ACS Sens. 3 (2018) 27–43.
[19] K. Kim, O.G. Tsay, D.A. Atwood, D.G. Churchill, Chem. Rev. 111 (2011) 5345–5403.
[20] X. Liu, N. Li, M. Li, et al., Coord. Chem. Rev. 404 (2020) 213109.
[21] B. Zhu, R. Sheng, T. Chen, et al., Coord. Chem. Rev. 463 (2022) 214527.
[22] Y.X. Tian, H.Y. Chen, J. Ma, et al., J. Hazard. Mater. 452 (2023) 131161.
[23] H. Ma, C. Wang, H. Suo, et al., Environ. Sci. Technol. 58 (2024) 17070–17080.
[24] X. Gao, Y. Lin, J. Li, et al., J. Hazard. Mater. 417 (2021) 125882.
[25] Y. Rui, X. Wu, B. Ma, Y. Xu, Chin. Chem. Lett. 29 (2018) 1387–1390.
[26] T. Islamoglu, M.A. Ortuno, E. Proussaloglou, et al., Angew. Chem. Int. Ed. 57 (2018) 1949–1953.
[27] J.N. Pearson, M. Patel, Ann. N. Y. Acad. Sci. 1378 (2016) 17–24.
[28] E.O. Freyre, A.T. Valencia, D.D. Guzmán, et al., Curr. Protein Pept. Sci. 22 (2021) 890–897.
[29] T.M.J.A. Moerenhout, J. Chen, H. Bouwmeester, et al., Environ. Sci. Technol. 58 (2024) 18834–18845.
[30] B. Yurash, H. Nakanotani, Y. Olivier, et al., Adv. Mater. 31 (2019) 1804490.
[31] D. Genovese, M. Cingolani, E. Rampazzo, et al., Chem. Soc. Rev. 50 (2021) 8414–8427.
[32] R. Gui, H. Jin, X. Bu, et al., Coord. Chem. Rev. 383 (2019) 82–103.
[33] X. Li, S. Zhao, B. Li, et al., Coord. Chem. Rev. 431 (2021) 213686.
[34] W. Sun, M. Li, J. Fan, X. Peng, Acc. Chem. Res. 52 (2019) 2818–2831.
[35] H. Niu, J. Liu, H.M. O'Connor, et al., Chem. Soc. Rev. 52 (2023) 2322–2357.
[36] W. Liu, K. Lv, C. Lu, et al., Chem. Eng. J. 498 (2024) 155457.
[37] L. Wu, C. Huang, B.P. Emery, et al., Chem. Soc. Rev. 49 (2020) 5110–5139.
[38] F. He, C. Nie, S. Liu, et al., Trends Food Sci. Technol. 148 (2024) 104490.
[39] A.C. Sedgwick, L. Wu, H.H. Han, et al., Chem. Soc. Rev. 47 (2018) 8842–8880.
[40] C.L. Chen, Y.T. Chen, A.P. Demchenko, P.T. Chou, Nat. Rev. Chem. 2 (2018) 131–143.
[41] V.S. Padalkar, S. Seki, Chem. Soc. Rev. 45 (2016) 169–202.
[42] X. Li, Y. Lv, S. Chang, et al., Anal. Chem. 91 (2019) 10927–10931.
[43] Z. Cheng, K.M. Fahy, G.W. Peterson, et al., Adv. Mater. 38 (2025) 2413848.
[44] H.H. Han, H. Tian, Y. Zang, et al., Chem. Soc. Rev. 50 (2021) 9391–9429.
[45] L.J. Fan, Y. Zhang, C.B. Murphy, et al., Coord. Chem. Rev. 253 (2009) 410–422.
[46] K.A. Van Houten, D.C. Heath, R.S. Pilato, J. Am. Chem. Soc. 120 (1998) 12359–12360.
[47] S.W. Zhang, T.M. Swager, J. Am. Chem. Soc. 125 (2003) 3420–3421.
[48] E.P. Lloyd, R.S. Pilato, K.A. Van Houten, ACS Omega 3 (2018) 16028–16034.
[49] A. Barba-Bon, A.M. Costero, S. Gil, et al., Chemistry 20 (2014) 6339–6347.
[50] R. Gotor, P. Gaviña, L.E. Ochando, et al., RSC Adv. 4 (2014) 15975–15982.
[51] R. Gotor, A.M. Costero, P. Gaviña, S. Gil, Dyes Pigm. 108 (2014) 76–83.
[52] Y. Liu, N. Guijarro, K. Sivula, Helv. Chim. Acta 103 (2020) e2000064.
[53] R. Huang, T. Liu, H. Peng, et al., Chem. Soc. Rev. 53 (2024) 6960–6991.
[54] T.-I. Kim, S.B. Maity, J. Bouffard, Y. Kim, Anal. Chem. 88 (2016) 9259–9263.
[55] Z. Lu, W. Fan, X. Shi, et al., Sens. Actuators B 255 (2018) 176–182.
[56] S. Huang, Y. Wu, F. Zeng, et al., J. Mater. Chem. C 4 (2016) 10105–10110.
[57] Y.C. Cai, C. Li, Q.H. Song, ACS Sens. 2 (2017) 834–841.
[58] P. Zheng, A. Abdurahman, Z. Zhang, et al., J. Hazard. Mater. 409 (2021) 124500.
[59] L. Zhang, K. Zhang, M. Wu, et al., Anal. Chem. 97 (2025) 3344–3351.
[60] L. Chen, H. Oh, D. Wu, et al., Chem. Commun. 54 (2018) 2276–2279.
[61] X. Zhou, Y. Zeng, C. Liyan, et al., Angew. Chem. Int. Ed. 55 (2016) 4729–4733.
[62] S. Jo, D. Kim, S.H. Son, et al., ACS Appl. Mater. Interfaces 6 (2014) 1330–1336.
[63] P. Zheng, A. Abdurahman, G. Liu, et al., Sens. Actuators B 322 (2020) 128611.
[64] H. Jiang, P. Wu, Y. Zhang, et al., Anal. Methods 9 (2017) 1748–1754.
[65] J.G. Weis, T.M. Swager, ACS Macro Lett. 4 (2015) 138–142.
[66] A. Balamurugan, H.I. Lee, Macromolecules 49 (2016) 2568–2574.
[67] W. Mo, Z. Zhu, F. Kong, et al., Nat. Commun. 13 (2022) 5189.
[68] Y.L. Pak, Y. Wang, Q. Xu, Coord. Chem. Rev. 433 (2021) 213745.
[69] Q. Shen, G. Song, H. Lin, et al., Adv. Mater. 36 (2024) 2310032.
[70] N. Duan, H. Wang, Y. Li, et al., Coord. Chem. Rev. 427 (2021) 213557.
[71] G.M. Calaf, Semin. Cancer Biol. 76 (2021) 206–217.
[72] R.D. Ayivi, S.O. Obare, J. Wei, TrAC Trends Anal. Chem. 167 (2023) 117231.
[73] Y. Cai, J. Fang, B. Wang, et al., Sens. Actuators B 292 (2019) 156–163.
[74] Q. Zhao, H. Mei, Y. Li, et al., Microchem. J. 169 (2021) 106541.
[75] J. Chang, H. Li, T. Hou, F. Li, Biosens. Bioelectron. 86 (2016) 971–977.
[76] Z. Wu, Z. Hao, Y. Chai, et al., Biosens. Bioelectron. 233 (2023) 115341.
[77] C. Tao, C. Wang, C. Zeng, et al., Food Chem. 482 (2025) 144143.
[78] X. Xu, W. Zhang, J. Huang, H. Xu, Trends Food Sci. Technol. 152 (2024) 104683.
[79] J. Wang, J. Zhang, J. Wang, et al., J. Hazard. Mater. 389 (2020) 122074.
[80] P. Sharma, M. Kumar, V. Bhalla, ACS Omega 5 (2020) 19654–19660.
[81] B. Zhang, J. Yan, Y. Shang, Z. Wang, Macromolecules 51 (2018) 1769–1776.
[82] B. Zhang, B. Li, Z. Wang, ACS Sensors 5 (2020) 162–170.
[83] H. Ren, S. Tai, A.O. Barimah, et al., Trends Food Sci. Technol. 152 (2024) 104682.
[84] G.L. Wei, D.Q. Li, M.N. Zhuo, et al., Environ. Pollut. 196 (2015) 29–46.
[85] A. Macan Schönleben, F. den Ouden, S. Yin, et al., Environ. Sci. Technol. 59 (2025) 9209–9220.
[86] J. Yang, Y. Yao, X. Li, et al., Environ. Sci. Technol. 58 (2024) 7986–7997.
[87] H. Zhu, Y. Xie, X. Zou, et al., Luminescence 37 (2021) 263–267.
[88] L. Shen, X. Huang, Z. Zhang, et al., Sci. Total Environ. 836 (2022) 155617.
[89] J. Hu, X. Zou, S. Ji, et al., Anal. Chim. Acta 1243 (2023) 340809.
[90] Y. Tian, X. Huang, H. Li, et al., Anal. Chim. Acta 1285 (2024) 342009.
[91] J. Singh, S. Thakur, R. Singh, V. Kaur, Food Chem. 327 (2020) 127080.
[92] S. Di Grande, I. Ciofini, C. Adamo, et al., J. Phys. Chem. A 126 (2022) 8809–8817.
[93] G.Y. Li, K.L. Han, WIREs Comput. Mol. Sci. 8 (2017) e1351.
[94] Y. Liu, M. Bouri, L. Yao, et al., Angew. Chem. Int. Ed. 60 (2021) 23651–23655.
[95] G. Díaz Mirón, M.C. González Lebrero, J. Phys. Chem. A 124 (2020) 9503–9512.

[96] Y. Liu, M. Xia, D. Ren, et al., ACS Energy Lett. 8 (2023) 1645–1651.
[97] C. Adamo, D. Jacquemin, Chem. Soc. Rev. 42 (2013) 845–856.
[98] Q. Chen, J. Liu, S. Liu, et al., Anal. Chem. 95 (2023) 4390–4394.
[99] L. Cui, Y. Gong, C. Cheng, et al., Adv. Sci. 8 (2021) 2002615.
[100] M.J. Sarmento, F. Fernandes, Fluoresc. Spectrosc. Microsc. Biol. (2022) 3–51.
[101] N. Wang, L. Zhang, J. Li, et al., Coord. Chem. Rev. 530 (2025) 216480.
[102] M. Zhang, Z. Chen, X. Liu, et al., J. Hazard. Mater. 452 (2023) 131177.
[103] M. Dai, Y.J. Yang, S. Sarkar, K.H. Ahn, Chem. Soc. Rev. 52 (2023) 6344–6358.
[104] K. Nawara, J. Waluk, Anal. Chem. 89 (2017) 8650–8655.
[105] Y. Zhu, X. Chong, Z. Luo, et al., J. Hazard. Mater. 472 (2024) 134604.